




# A Theory of Spherical Diagrams

Giovanni Viglietta   

School of Information Science, Japan Advanced Institute of Science and Technology (JAIST), Japan

---

## Abstract

We introduce the axiomatic theory of Spherical Occlusion Diagrams as a tool to study certain combinatorial properties of polyhedra in  $\mathbb{R}^3$ , which are of central interest in the context of Art Gallery problems for polyhedra and other visibility-related problems in discrete and computational geometry.

**Keywords and phrases** Spherical Occlusion Diagram, polyhedron, visibility, Art Gallery problem, swirl graph

**Acknowledgements** The author is grateful to C. D. Tóth, J. Urrutia, and M. Yamashita for interesting discussions. The author also thanks the anonymous reviewers of CCCG 2022 for useful suggestions.

## 1 Introduction

### Geometric intuition

Consider a set  $\mathcal{P}$  of internally disjoint opaque polygons in  $\mathbb{R}^3$  and a viewpoint  $v \in \mathbb{R}^3$  such that no vertex of any polygon in  $\mathcal{P}$  is visible to  $v$ . An example is given by the set of six rectangles in Figure 1 (left) with respect to the point  $v$  located at the center of the arrangement.

Let  $S$  be a sphere centered at  $v$  that does not intersect any of the polygons in  $\mathcal{P}$  (we may assume without loss of generality that  $S$  is the unit sphere), and let  $S_{\mathcal{P}}$  be the *visibility map* of  $\mathcal{P}$  with respect to  $v$ . That is,  $S_{\mathcal{P}}$  is the set of radial projections onto  $S$  of the portions of edges of polygons in  $\mathcal{P}$  that are visible to  $v$  (i.e., where polygons occlude projection rays). Figure 1 (right) shows an example of such a projection. The resulting structure  $S_{\mathcal{P}}$  is a *Spherical Occlusion Diagram*; this name indicates the fact that no vertices of  $\mathcal{P}$  appear in the visibility map, because they are all occluded by polygons.

In this paper we set out to formalize an axiomatic theory of Spherical Occlusion Diagrams and study their combinatorial structure.

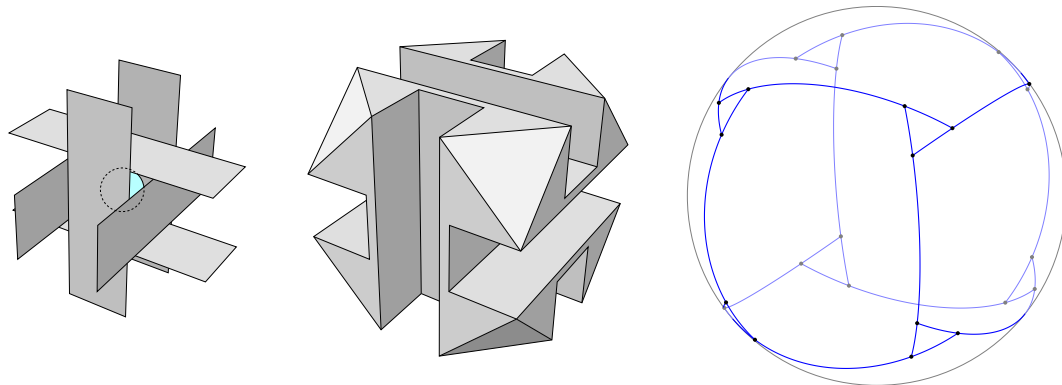


**Figure 1** Construction of a Spherical Occlusion Diagram (right) as the visibility map of an arrangement of six rectangles (left) or the visibility map of a polyhedron with respect to the central point, which does not see any vertices (center)

### Applications

Spherical Occlusion Diagrams naturally arise in visibility-related problems for arrangements of polygons in  $\mathbb{R}^3$ , and especially for polyhedra.

An example is found in [3], where an upper bound is given on the number of edge guards that solve the Art Gallery problem in a general polyhedron. That is, given a polyhedron  $\mathcal{P}$ , the problem is to find a (small) set of edges that collectively see the whole interior of  $\mathcal{P}$ . An edge  $e$  sees a point  $x$  if and only if there is a point  $y \in e$  such that the open line segment  $xy$  does not intersect the boundary of  $\mathcal{P}$ . (The reader can refer to [2, 11] for more results on this problem, as well as [7] for a survey on the Art Gallery problem in 2-dimensional settings.)

The idea of [3] is to preliminarily select a (small) set  $E$  of edges that cover all vertices of  $\mathcal{P}$ . Note that  $E$  may be insufficient to guard the interior of  $\mathcal{P}$ , as some of its points may be invisible to all vertices; Figure 1 (center) shows an example. Thus, an additional (small) set of edges  $E'$  is selected, which collectively see all internal points of  $\mathcal{P}$  that do not see any vertices. Clearly,  $E \cup E'$  is a set of edges that see all internal points of  $\mathcal{P}$ .

The selection of the set of edges  $E'$  is carried out in [3] by means of an ad-hoc analysis of some properties of points that do not see any vertices of  $\mathcal{P}$ . Spherical Occlusion Diagrams offer a systematic and general tool to reason about points in a polyhedron that do not see any vertices.

Spherical Occlusion Diagrams have also provided a framework for proving the main result of [9, 10]: Any point that sees no vertex of a polyhedron must see at least 8 of its edges, and the bound is tight.

### Summary

In Section 2 we give an axiomatic theory of Spherical Occlusion Diagrams and discuss their realizability as visibility maps. In Section 3 we prove some basic properties of Spherical Occlusion Diagrams, while in Section 4 we focus on an important pattern called *swirl*. Sections 5 and 6 are devoted to two interesting classes of Spherical Occlusion Diagrams: the *swirling* and the *uniform* ones, respectively. Section 7 contains some concluding remarks and directions for future research.

A preliminary version of this paper appeared at CCCG 2022 [12]. In the present version, most sections have been reworked and all missing proofs have been included. In addition, Proposition 13 and Theorem 25 are new contributions.

## 2 Axiomatic theory

In the following, we will abstract from a specific set of polygons  $\mathcal{P}$  and a viewpoint  $v$ , and we will focus on the salient properties of the Spherical Occlusion Diagrams constructed in Section 1 in order to devise a small set of axioms that describe all of them.

### Definitions

Some terms will be useful. A *great circle* on a sphere  $S$  is a circle of maximum diameter within  $S$ . Equivalently, a great circle is the intersection between  $S$  and a plane through its center. Two points on a sphere are *antipodal* if the line through them contains the center of the sphere. A *great semicircle* is an arc of a great circle whose endpoints are antipodal.

The *geodesic arc* between two distinct non-antipodal points  $x$  and  $y$  on a sphere  $S$  is the unique shortest path within  $S$  having endpoints  $x$  and  $y$ . Equivalently, it is the arc of the

unique great circle through  $x$  and  $y$  that has  $x$  and  $y$  as endpoints and is strictly shorter than a great semicircle. Two geodesic arcs are *collinear* if they lie on the same great circle.

► **Definition 1.** Let  $a$  and  $b$  be two non-collinear geodesic arcs on a sphere. If an endpoint  $p$  of  $a$  lies in the relative interior of  $b$ , we say that  $a$  hits  $b$  at  $p$  (or feeds into  $b$  at  $p$ ) and  $b$  blocks  $a$  at  $p$ .

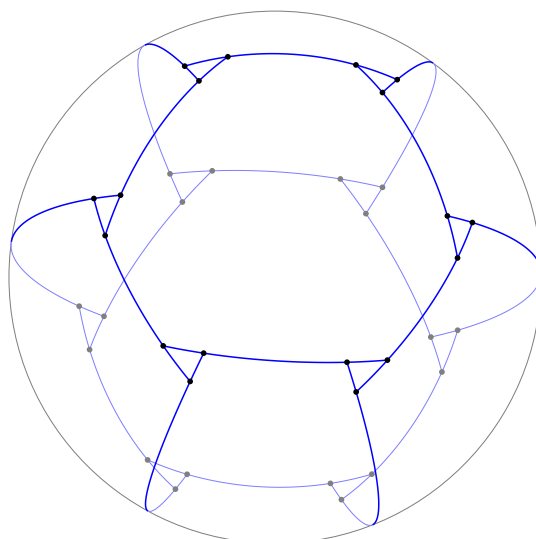
### Axioms

We are now ready to formulate an abstract theory of Spherical Occlusion Diagrams.

► **Definition 2.** A Spherical Occlusion Diagram (SOD) is a finite non-empty collection  $\mathcal{D}$  of geodesic arcs on the unit sphere in  $\mathbb{R}^3$  satisfying the following axioms.

- A1. Any two arcs in  $\mathcal{D}$  are internally disjoint.
- A2. Each arc in  $\mathcal{D}$  is blocked by arcs of  $\mathcal{D}$  at each endpoint.
- A3. All arcs in  $\mathcal{D}$  that hit the same arc of  $\mathcal{D}$  reach it from the same side.

As an example, Figure 2 shows a SOD with 18 arcs.



■ **Figure 2** Example of a SOD with 18 arcs

### Discussion

We remark that the SOD axioms introduced in [12] are slightly different. In particular, the axiom A1 therein states that, if two arcs  $a, b \in \mathcal{D}$  have a non-empty intersection, then  $a$  hits  $b$  or  $b$  hits  $a$ . Also, in [12] it is not postulated that arcs are shorter than great semicircles, but this property is derived as a theorem.

The axioms in the present paper are slightly more inclusive, in that they allow multiple arcs to share an endpoint, as long as the common endpoint is an interior point of some other arc. Allowing such “degenerate configurations” in SODs allows us to prove a slightly more general Proposition 3, whereas the one in [12] required the extra assumption that the viewpoint  $v$  be in “general position” with respect to the polyhedron  $\mathcal{P}$ .

Moreover, if we removed the assumption that the arcs in a SOD are shorter than great semicircles, we would still be able to prove that arcs are *not longer* than great semicircles, but this would not exclude some degenerate cases in which some arcs are great semicircles.

### Realizability

It is easy to recognize that the SODs  $S_{\mathcal{P}}$  as constructed in Section 1 indeed provide a model for our theory, as they satisfy all its axioms, at least when  $\mathcal{P}$  is a polyhedron.

► **Proposition 3.** *The visibility map  $S_{\mathcal{P}}$  of any polyhedron  $\mathcal{P}$  with respect to any viewpoint  $v$  that sees no vertices of  $\mathcal{P}$  satisfies the axioms of Spherical Occlusion Diagrams.*

**Proof.** For each arc  $a \in S_{\mathcal{P}}$ , let  $e_a$  be the edge of  $\mathcal{P}$  whose radial projection on the sphere (partly occluded by faces of  $\mathcal{P}$ ) contains  $a$ . Since  $e_a$  is a line segment of finite length,  $a$  must be an arc of a great circle that is shorter than a great semicircle, i.e., a geodesic arc.

Also, since  $e_a$  is an edge of a face  $F \in \mathcal{P}$  that is partially visible to  $v$ , all arcs of  $S_{\mathcal{P}}$  that touch the interior of  $a$  must reach it from the same side (axiom A3) and cannot continue past  $a$  (axiom A1), because such arcs correspond to edges partially hidden by  $F$  (hence,  $e_a$  must be a reflex edge of  $\mathcal{P}$ ).

Finally, the fact that each vertex of  $\mathcal{P}$  is occluded by some face translates into the property that each endpoint of each arc in  $S_{\mathcal{P}}$  must lie in the interior of another arc of  $S_{\mathcal{P}}$  (axiom A2). ◀

Note that Proposition 3 also holds (with the same proof) for any arrangement  $\mathcal{P}$  of internally disjoint polygons, none of which is coplanar to the viewpoint  $v$ .

It is known that the converse of Proposition 3 is not true, as not every SOD is the visibility map of a polyhedron [5]. There is also compelling evidence that a stronger statement holds, which we state next.

► **Definition 4.** *A SOD  $\mathcal{D}$  is irreducible if no proper subset of  $\mathcal{D}$  is a SOD.*

► **Conjecture 5.** *There is an irreducible Spherical Occlusion Diagram (satisfying the conditions in Definition 2) that is not the visibility map  $S_{\mathcal{P}}$  of any polyhedron  $\mathcal{P}$  with respect to any viewpoint  $v$  that sees no vertices of  $\mathcal{P}$ .*

We remark that Conjecture 5 automatically extends to arbitrary arrangements  $\mathcal{P}$  of disjoint polygons; actually, it is sufficient to prove Conjecture 5 for *simply connected* polyhedra. Indeed, a set of disjoint polygons  $\mathcal{P}$  that gives rise to a SOD  $\mathcal{D}$  with respect to a viewpoint  $v$  can easily be augmented by adding a mesh of polygons whose edges are either shared with  $\mathcal{P}$  or concealed from  $v$  by polygons in  $\mathcal{P}$ . The resulting simply connected polyhedron gives rise to the same SOD  $\mathcal{D}$  (a possible way of implementing this construction is found in [10]).

## 3 Elementary properties

We will prove some basic properties of SODs. In fact, all theorems in this section hold more generally for finite non-empty collections of geodesic arcs that satisfy axioms A1 and A2, but not necessarily A3.

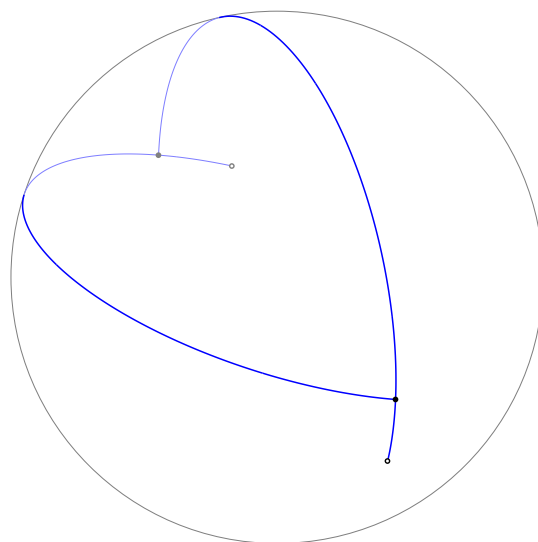
It is immediate to prove a stronger form of axiom A2.

► **Proposition 6.** *Every arc in a SOD hits exactly two distinct arcs, one at each endpoint.*

**Proof.** Let  $p$  be an endpoint of an arc  $a$ . By axiom A2,  $a$  hits at least one arc  $b$  at  $p$ . If  $a$  hit a second arc  $b'$  at  $p$ , then  $p$  would be interior to both  $b$  and  $b'$ , contradicting axiom A1. ◀

► **Proposition 7.** *No two arcs in a SOD intersect in more than one point.*

**Proof.** Two internally disjoint arcs sharing two points cannot be shorter than great semicircles, contradicting the assumption that a SOD consists of geodesic arcs (see Figure 3). ◀



■ **Figure 3** Two non-collinear arcs can only intersect in two antipodal points.

For the next results, we describe a general construction called “monotonic walk”; refer to Figure 4. Let  $\mathcal{D}$  be a SOD, and let  $p$  and  $p'$  be antipodal points on the unit sphere. A *clockwise monotonic walk around  $p$*  starting from a point  $x_0 \notin \{p, p'\}$  on an arc  $a_0 \in \mathcal{D}$  is a sequence of pairs  $(x_i, a_i)$ , where  $x_i \in a_i \in \mathcal{D}$  for all  $i \geq 0$ , defined inductively as follows. Assuming  $x_i$  is a point of  $a_i \in \mathcal{D}$  distinct from  $p$  and  $p'$ , we distinguish two cases. If the great circle containing  $a_i$  also contains  $p$  and  $p'$ , then  $x_{i+1}$  is an endpoint of  $a_i$  such that the geodesic arc  $x_i x_{i+1}$  contains neither  $p$  nor  $p'$  (such an endpoint must exist, or else  $a_i$  would not be shorter than a great semicircle; in the special case where  $x_i$  is an endpoint of  $a_i$ , we take  $x_{i+1} = x_i$ ). Otherwise, the great circle containing  $a_i$  separates  $p$  from  $p'$ . Following this great circle in the clockwise direction with respect to  $p$  starting at  $x_i$ , we define  $x_{i+1}$  as the first endpoint of  $a_i$  encountered. In both cases, we let  $a_{i+1}$  be the (unique, due to Proposition 6) arc of  $\mathcal{D}$  that blocks  $a_i$  at  $x_{i+1}$ .

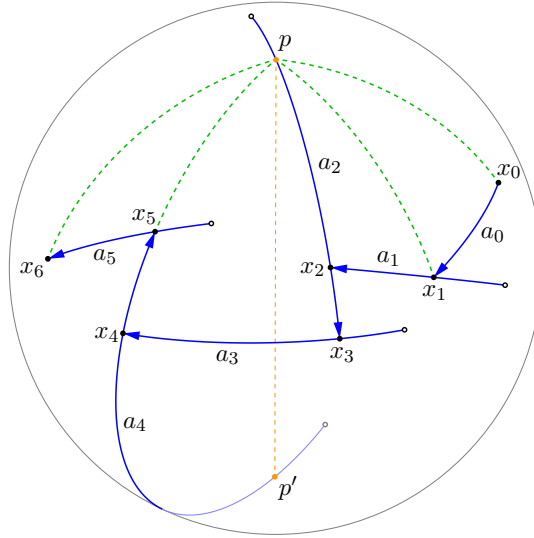
A *counterclockwise monotonic walk* around a point is defined similarly.

► **Proposition 8.** *Given a SOD  $\mathcal{D}$ , the relative interior of any great semicircle on the unit sphere intersects some arc of  $\mathcal{D}$ .*

**Proof.** Let  $p$  and  $p'$  be the (antipodal) endpoints of a great semicircle  $c$ . Since  $\mathcal{D}$  is not empty, there exists an arc  $a_0 \in \mathcal{D}$ . Recall that the endpoints of a geodesic arc are distinct; therefore,  $a_0$  contains infinitely many points, and in particular it contains a point  $x_0$  distinct from  $p$  and  $p'$ . Consider a clockwise monotonic walk  $((x_i, a_i))_{i \geq 0}$  around  $p$  starting from  $x_0$ . Observe that any  $a_i$  that is an arc of a great circle through  $p$  and  $p'$  must be followed by an arc  $a_{i+1}$  that is not. Hence, the monotonic walk makes steady progress around  $p$ . Since  $\mathcal{D}$  is finite, in a finite amount of steps the monotonic walk touches the interior of every great semicircle with endpoints  $p$  and  $p'$ , including  $c$ . ◀

► **Proposition 9.** *A SOD partitions the unit sphere into spherically convex regions.*

**Proof.** Let  $\mathcal{D}$  be a SOD on the unit sphere  $S$ , let  $D$  be the union of the arcs in  $\mathcal{D}$ , and let  $p$  and  $q$  be two points in the same connected component of  $S \setminus D$ . We will prove that  $p$  and  $q$  are connected by a single geodesic arc that does not intersect  $D$ .



■ **Figure 4** The initial steps of a clockwise monotonic walk around  $p$  starting from  $x_0 \in a_0$

By assumption and by the finiteness of  $\mathcal{D}$ , there is a chain  $C$  consisting of  $k$  geodesic arcs (drawn in green in Figure 5) that connects  $p$  and  $q$  without intersecting  $D$ . Let us choose  $C$  so that  $k$  is minimum. If  $k = 1$ , there is nothing to prove. Thus, assume that  $k \geq 2$ .

Let  $pp'$  and  $p'p''$  be the first two geodesic arcs of  $C$ . If  $p$  and  $p''$  are antipodal, then  $pp'$  and  $p'p''$  are collinear, and their union is a great semicircle. By Proposition 8,  $D$  intersects  $pp' \cup p'p''$ , which is a contradiction. Hence  $p$  and  $p''$  are not antipodal, and there is a unique geodesic arc  $pp''$  (drawn in orange).

Assume for a contradiction that  $D$  intersects  $pp''$  in  $x \notin \{p, p''\}$ . Then, either a clockwise or a counterclockwise monotonic walk around  $p$  starting from  $x$  must intersect  $pp' \cup p'p''$ , which is again a contradiction (see Figure 5). Therefore,  $D$  does not intersect  $pp''$ , and we can replace  $pp'$  and  $p'p''$  in  $C$  by the single geodesic arc  $pp''$ . Since this contradicts the minimality of  $k$ , we conclude that  $k = 1$ . ◀

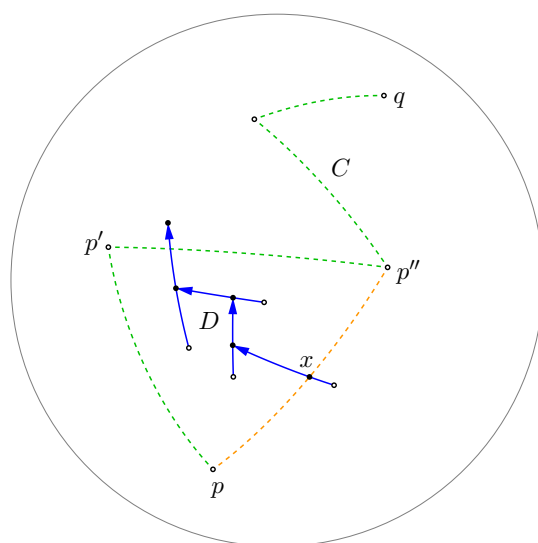
► **Definition 10.** Each of the spherically convex regions into which the unit sphere is partitioned by a SOD is called a tile.

► **Corollary 11.** In a SOD, no tile (including its boundary) contains two antipodal points.

**Proof.** If two antipodal points  $p$  and  $p'$  were in a same tile  $T$  (or on its boundary), then by Proposition 9 there would be a great semicircle with endpoints  $p$  and  $p'$  whose interior is entirely contained in  $T$ . However, this would contradict Proposition 8. ◀

► **Lemma 12.** A simple closed curve on the unit sphere cannot be decomposed into two geodesic arcs.

**Proof.** Assume for a contradiction that a simple closed curve is the concatenation of two geodesic arcs  $g_1$  and  $g_2$ , both with endpoints  $p_1$  and  $p_2$ . If  $g_1$  and  $g_2$  are not collinear, then both are great semicircles, because they share the two points  $p_1$  and  $p_2$ , which must be antipodal (see Figure 3). This contradicts the fact that  $g_1$  and  $g_2$  are geodesic arcs. If, on the other hand,  $g_1$  and  $g_2$  are collinear, then their concatenation must be a great circle. This implies that at least one of them, say  $g_1$ , is at least as long as a great semicircle, which is again a contradiction. ◀



■ **Figure 5** Proof of Proposition 9: The chain  $C$  can be simplified by connecting  $p$  and  $p''$ .

The following result states that the *contact graph* of a SOD is 3-connected.

► **Proposition 13.** *Removing any two arcs from a SOD and taking the union of the remaining arcs yields a connected subset of the unit sphere.*

**Proof.** Let  $\mathcal{D}$  be a SOD, let  $a, b \in \mathcal{D}$ , and let  $D$  be the union of all arcs of  $\mathcal{D}$  other than  $a$  and  $b$ . Assume for a contradiction that  $D$  is not connected. Thus, there exists a closed curve  $\gamma$  on the unit sphere that does not intersect  $D$  and separates it into two non-empty sets. It follows that  $\gamma$  intersects no arcs of  $\mathcal{D}$  other than  $a$  and  $b$ , and hence it touches at most two tiles of  $\mathcal{D}$ .

Note that  $\gamma$  cannot intersect only one tile  $T$ , otherwise there would be an arc, say  $a$ , that has the same tile  $T$  on both sides, violating Proposition 9. So,  $\gamma$  intersects exactly two tiles  $T_1$  and  $T_2$ , both of which are incident to  $a$  and  $b$ . In fact, there is a point  $p_1 \in a$  (respectively,  $p_2 \in b$ ) on the common boundary between  $T_1$  and  $T_2$ . By Corollary 11, there is a geodesic arc  $g_1$  (respectively,  $g_2$ ) with endpoints  $p_1$  and  $p_2$ , entirely contained in  $T_1$  (respectively,  $T_2$ ). The concatenation of  $g_1$  and  $g_2$  is a simple closed curve, which is impossible due to Lemma 12. We conclude that  $D$  is connected. ◀

► **Corollary 14.** *The union of all the arcs in a SOD is a connected set.*

**Proof.** Immediate from Proposition 13. ◀

There is a very clean relationship between the number of arcs in a SOD and the number of tiles: There are two more tiles than there are arcs.

► **Proposition 15.** *A SOD with  $n$  arcs partitions the unit sphere into  $n + 2$  tiles.*

**Proof.** Every endpoint of an arc of a SOD divides the arc it hits into two sub-arcs. The set of these sub-arcs induces a spherical drawing of a planar graph with  $k$  vertices and  $n + k$  edges. Each face of this drawing coincides with a tile of the SOD. By Euler's formula, the number of faces is  $(n + k) - k + 2 = n + 2$ . ◀

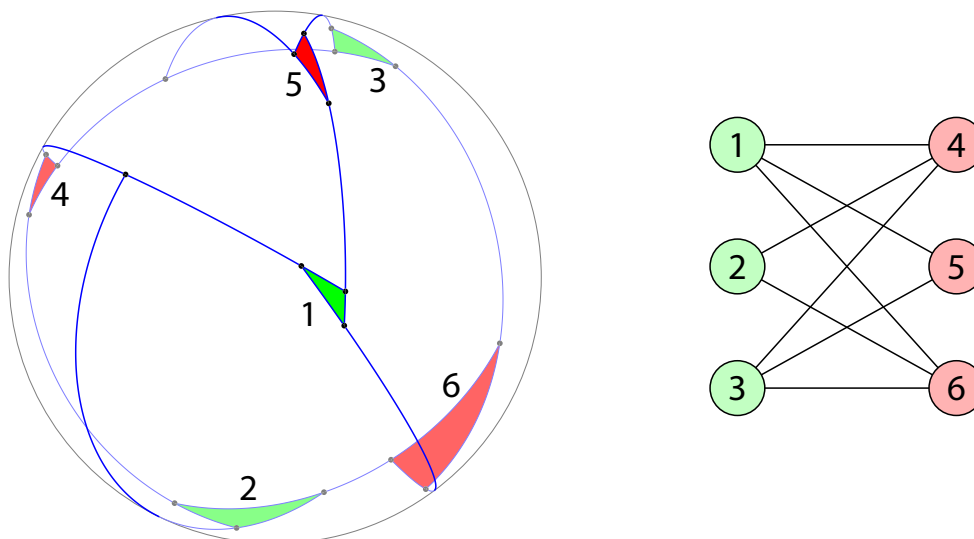
#### 4 Swirls

There is a curious similarity between SODs and continuous vector fields on a sphere. According to the hairy ball theorem, “it is impossible to comb a hairy ball without creating cowlicks”. Similarly, it is impossible to construct a SOD without creating “swirls”, as we shall see in this section.

► **Definition 16.** A swirl in a SOD is a cycle of arcs, each of which feeds into the next, going either all clockwise or all counterclockwise. The spherically convex region enclosed by a swirl is called the eye of that swirl.

Figure 2 shows a SOD with six clockwise swirls and six counterclockwise swirls. Observe that, in an irreducible SOD, the eye of each swirl coincides with a single tile; in general, the eye of a swirl is a union of tiles, as it may have internal arcs.

► **Definition 17.** The swirl graph of a SOD  $\mathcal{D}$  is the undirected multigraph on the set of swirls of  $\mathcal{D}$  having an edge between two swirls for every arc in  $\mathcal{D}$  shared by the two swirls.



■ **Figure 6** A SOD and its swirl graph

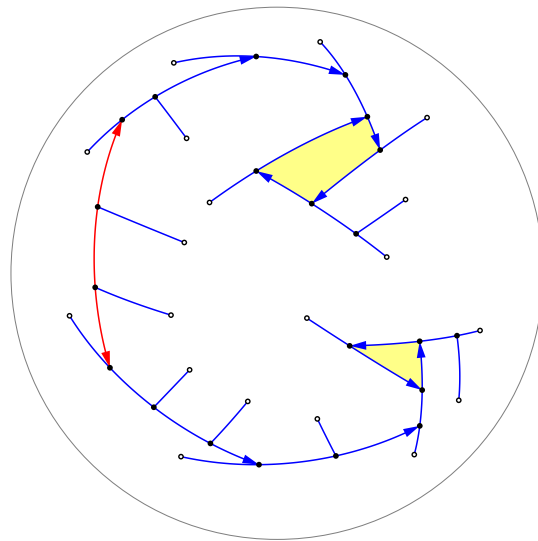
In Figure 6, the eyes of clockwise swirls are colored green, and the eyes of counterclockwise swirls are colored red. Observe that the swirl graph is simple and bipartite; this is true in general, as the next theorem shows. (Note that for the first time we will be using axiom A3.)

► **Theorem 18.** The swirl graph of any SOD is a simple planar bipartite graph with non-empty partite sets.

**Proof.** The swirl graph is spherical, hence planar. It is bipartite, where the partite sets correspond to clockwise and counterclockwise swirls, respectively. Indeed, if the same arc is shared by two concordant swirls (say, clockwise), then it is hit by arcs from both sides, violating axiom A3.

Figure 7 shows how to find a clockwise and a counterclockwise swirl in any SOD. For a clockwise swirl, start from any arc and follow it in any direction until it hits another arc. Then turn clockwise and follow this arc until it hits another arc, and so on. The sequence

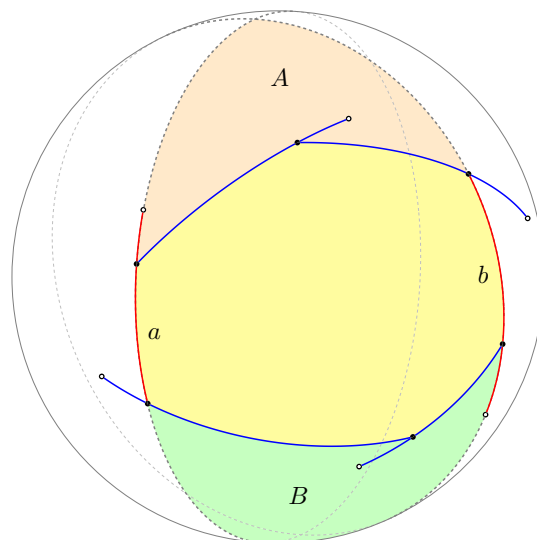




■ **Figure 7** Finding swirls in a SOD

of arcs encountered is eventually periodic, and the period identifies a clockwise swirl. A counterclockwise swirl is found in a similar way.

To prove that the swirl graph is simple, assume for a contradiction that a swirl  $\mathcal{S}_1$  shares two arcs  $a$  and  $b$  with another swirl  $\mathcal{S}_2$ . Then, the eye of  $\mathcal{S}_2$  must be entirely contained in the spherical lune determined by  $a$  and  $b$ , as shown in Figure 8. Since the eye of  $\mathcal{S}_2$  is bounded by  $a$ , it must lie in the region  $A$ . However, the eye of  $\mathcal{S}_2$  is also bounded by  $b$ , and thus it must lie in the region  $B$ . This is a contradiction, since  $A$  and  $B$  are disjoint. ◀

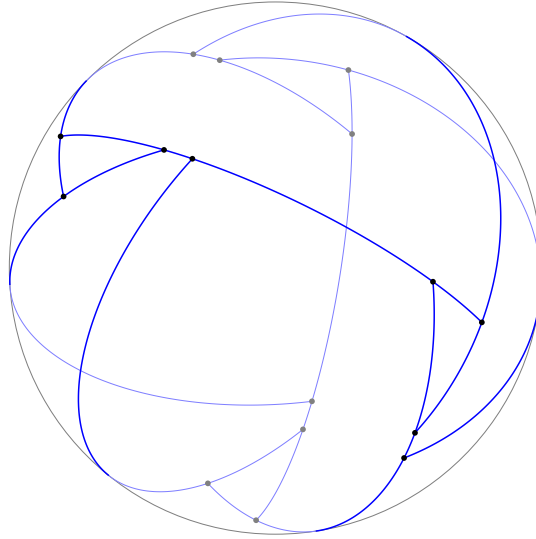


■ **Figure 8** Two swirls cannot share more than one arc.

More is actually known about swirl graphs.

► **Theorem 19.** *Every SOD has at least four swirls.* ◀

This result has been announced in [9], and a proof can be found in [10]. From Theorem 19, it easily follows that every SOD has at least eight arcs. On the other hand, Figure 9 shows an example of a SOD with exactly eight arcs and exactly four swirls, which is therefore minimal.



■ **Figure 9** A SOD with eight arcs and four swirls

It is not yet clear whether there are SODs with only one clockwise swirl (or only one counterclockwise swirl), but there is overwhelming evidence that this is not the case.

► **Conjecture 20.** *Every SOD has at least two clockwise and two counterclockwise swirls.*

## 5 Swirling SODs

This section is devoted to a special type of SODs whose arcs always meet forming swirls. Patterns arising in these SODs are found in modular origami, globe knots, rattan balls, etc.

► **Definition 21.** *A SOD is swirling if every arc is part of two swirls.*

An example of a swirling SOD is found in Figure 2; further examples are in Figure 14. All of these SODs were obtained from convex polyhedra or, more precisely, from convex subdivisions of the sphere, by a process that we call *swirlification*. As we will see in this section, there is a deep relationship between convex polyhedra and swirling SODs.

A *convex subdivision* of the unit sphere is a partition into spherically convex polygons called *faces* by a finite set of geodesic arcs called *edges*. The graph induced by the edges is called the *1-skeleton* of the convex subdivision. Note that the visibility map of a convex polyhedron with respect to an internal point is the 1-skeleton of a convex subdivision of the unit sphere.

► **Definition 22.** *A swirlable subdivision of the unit sphere is a convex subdivision where each face has an even number of edges.*

► **Proposition 23.** *A convex subdivision of the unit sphere is swirlable if and only if its 1-skeleton is bipartite.*

**Proof.** The 1-skeleton is bipartite if and only if it has no odd cycles, which is true if and only if each face has an even number of edges. ◀

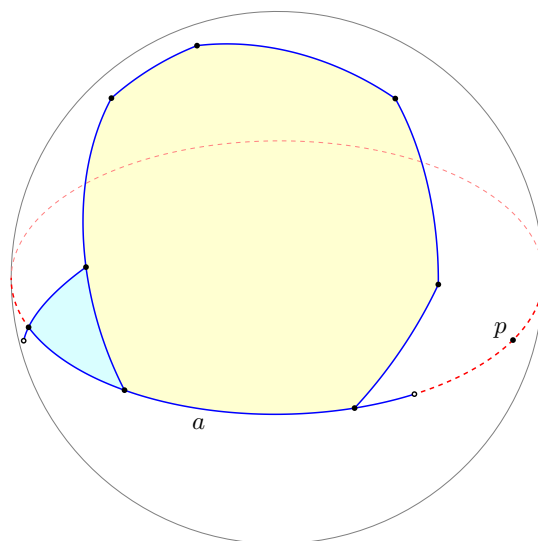
Given a swirlable subdivision of the sphere, the operation of turning each of its vertices into a swirl, going clockwise or counterclockwise according to the bipartition of the 1-skeleton, is called *swirlification*. As we will prove next, the swirlification operation allows us to turn any swirlable subdivision of the sphere into a swirling SOD. In fact, we will prove something more: The swirl graphs of swirling SODs are precisely the 1-skeletons of convex polyhedra with even-sided faces. Note that, by a well-known theorem of Steinitz, these graphs can be characterized as the 3-vertex-connected planar bipartite graphs.<sup>1</sup>

► **Lemma 24.** *In a SOD, let  $U$  be (the closure of) the union of two adjacent tiles, one of which is the eye of a swirl. Then,  $U$  is entirely contained in the interior of a hemisphere.*

**Proof.** Since one of the two adjacent tiles is the eye of the swirl, there is an arc  $a$  of the SOD that is shared by the boundaries of both tiles, as shown in Figure 10. Since the tiles of a SOD are spherically convex (Proposition 9),  $a$  bounds a hemisphere  $H$  containing both tiles.

We claim that  $U \cap a = U \cap \partial H$ , where  $\partial H$  is the great circle bounding  $H$ . Obviously  $U \cap a \subseteq U \cap \partial H$  because  $a \subseteq \partial H$ ; we have to prove that  $U \cap \partial H \subseteq U \cap a$ . Assume for a contradiction that there is a point  $p \in U \cap (\partial H \setminus a)$ , as shown in Figure 10. Since  $p \in U$ , it lies on the boundary of one of the two tiles, say  $T$ . Let  $p'$  be any point of  $a$  located on the boundary of  $T$  such that  $p$  and  $p'$  are not antipodal. By the convexity of  $T$ , the geodesic arc  $pp' \subset H$  is part of the boundary of  $T$ . Since  $pp'$  is collinear with  $a$  and intersects it, it must be part of  $a$ . Thus, we reach the contradiction that  $p \in a$ .

We have proved that  $U \cap a = U \cap \partial H$ . Therefore, translating the center of  $H$  slightly toward the center of  $a$  yields a hemisphere whose interior contains  $U$ . ◀



■ **Figure 10** The eye of a swirl and an adjacent tile share an arc  $a$ .

Observe that Proposition 13 immediately implies that the swirl graph of a swirling SOD is 3-edge-connected. The following theorem greatly strengthens this result.

► **Theorem 25.** *A graph is the swirl graph of a swirling SOD if and only if it is a 3-vertex-connected planar bipartite graph.*

<sup>1</sup> Steinitz's theorem states that a graph  $G$  can be realized as the 1-skeleton of a convex polyhedron if and only if  $G$  is 3-vertex-connected and planar.

**Proof.** Let  $G$  be a 3-vertex-connected planar bipartite graph. We will construct a swirling SOD whose swirl graph is  $G$ . By Steinitz's theorem, there is a convex polyhedron  $\mathcal{P}$  whose 1-skeleton is isomorphic to  $G$ . Radially projecting the 1-skeleton of  $\mathcal{P}$  onto a sphere whose center is internal to  $\mathcal{P}$  yields a swirable subdivision  $\mathcal{S}$  of the sphere, due to Proposition 23 and the convexity of  $\mathcal{P}$ . Note that the 1-skeleton of  $\mathcal{S}$  is  $G$ , as well.

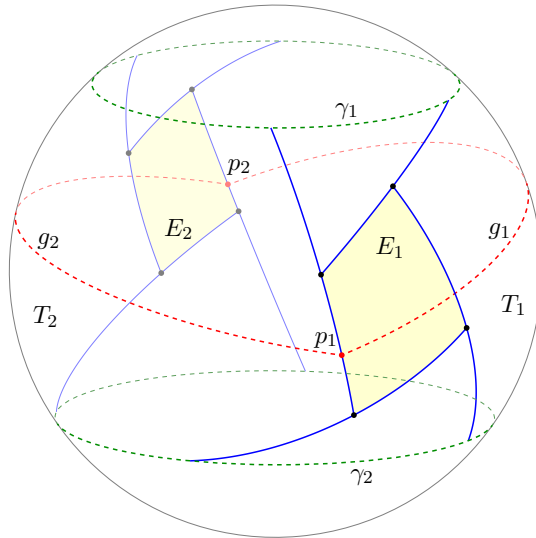
Since each edge of  $\mathcal{S}$  is a geodesic arc, we can perturb its endpoints within a small-enough  $\epsilon$ -neighborhood without making them antipodal. This operation allows us to create a small swirl in lieu of each vertex of  $\mathcal{S}$ , while moving each edge by at most  $\epsilon$  (this is possible in particular because the faces of  $\mathcal{S}$  are convex, and hence do not have reflex angles). If the swirls go clockwise or counterclockwise according to the bipartition of the 1-skeleton of  $\mathcal{S}$ , and if  $\epsilon$  is small enough, the resulting set of geodesic arcs is a swirling SOD. Since every arc in a swirling SOD is an edge of its swirl graph, the swirl graph must be  $G$ .

Conversely, let  $G$  be the swirl graph of a swirling SOD. By Theorem 18,  $G$  is planar and bipartite. It remains to prove that  $G$  is 3-vertex-connected. We know there are at least four swirls (Theorem 19); we want to prove that removing any two of them does not disconnect the swirl graph. Equivalently, since the SOD is swirling, removing the arcs constituting two swirls  $S_1$  and  $S_2$  does not disconnect the SOD.

Assume the contrary, and let  $E_1$  and  $E_2$  be the eyes of  $S_1$  and  $S_2$ , respectively, as shown in Figure 11. By assumption, removing  $S_1$  and  $S_2$  causes the SOD to disconnect. Thus, there is a region  $R$  of the sphere bounded by two disjoint simple closed curves  $\gamma_1$  and  $\gamma_2$  such that  $E_1 \cup E_2 \subset R$  and no arcs of the SOD other than those of  $S_1$  and  $S_2$  intersect the interior of  $R$ .

Therefore, as Figure 11 shows, there are two tiles  $T_1$  and  $T_2$ , located on opposite sides of  $R$ , each of which is adjacent to both  $E_1$  and  $E_2$ . In the special case where  $S_1$  and  $S_2$  share an arc (more than one is impossible, due to Theorem 18), there are three such tiles, two of them on the same side of  $R$ .

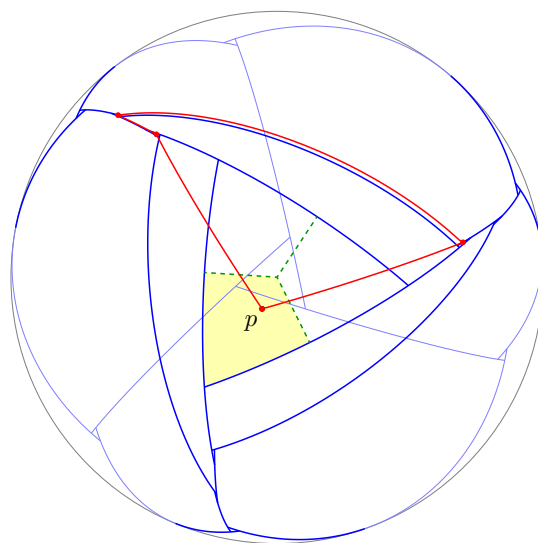
Let  $p_1$  (respectively,  $p_2$ ) be a point on the common boundary between  $E_1$  and  $T_2$  (respectively,  $E_2$  and  $T_1$ ). Due to Lemma 24, there are two geodesic arcs  $g_1$  and  $g_2$ , both with endpoints  $p_1$  and  $p_2$ , such that the concatenation of  $g_1$  and  $g_2$  is a simple closed curve. Since this contradicts Lemma 12, we conclude that  $G$  is 3-vertex-connected.  $\blacktriangleleft$



■ **Figure 11** Proof of Theorem 25: Removing the two swirls disconnects the SOD.

We might be tempted to reverse the swirlification operation by “contracting” the eye of each swirl of a swirling SOD into an interior point in order to obtain a swirable subdivision of the sphere. Unfortunately, this is not always possible, and Figure 12 shows an example. The example shows a swirling SOD with a 3-fold rotational symmetry around the center of a large triangular eye  $E$ . Replace the eye of each swirl with an interior point, and move the arcs of the SOD accordingly to form a subdivision of the sphere. No matter how an interior point  $p \in E$  is chosen, the subdivision always has a non-convex face (the boundary of such a face is drawn in red in Figure 12).

Nonetheless, Theorem 25 implies that it is always possible to contract the eyes of all swirls to (not necessarily interior) points to obtain a swirable (hence convex) subdivision of the sphere. This fact was also suggested, without proof, in [12].



■ **Figure 12** Contracting the eye of each swirl into an interior point necessarily yields a non-convex subdivision of the sphere.

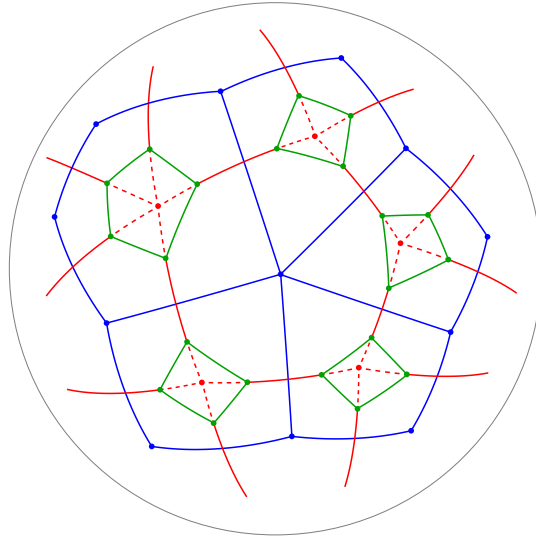
Note that we can also obtain a swirable subdivision of the sphere by taking the dual of a subdivision whose vertices have even degree, or by truncating it. More generally, we have the following.

► **Proposition 26.** *A convex subdivision of the sphere is swirable if and only if its truncated dual is swirable.*

**Proof.** Observe that the operations of truncation and taking the dual of a convex subdivision of the sphere preserve the convexity of the subdivision. To conclude the proof, we only have to show that a convex subdivision has even-sided faces if and only if its truncated dual does.

Figure 13 illustrates the procedure of truncating the dual of a convex subdivision  $\mathcal{S}_1$  of the sphere. The edges of  $\mathcal{S}_1$  are drawn in blue, and the ones in red are the edges of its dual  $\mathcal{S}_2$ . Note that  $\mathcal{S}_2$  has a vertex in each face of  $\mathcal{S}_1$ , and vice versa. Moreover, the degree of each vertex of  $\mathcal{S}_2$  is equal to the number of edges of the face of  $\mathcal{S}_1$  containing it. Truncating  $\mathcal{S}_2$  amounts to drawing the green edges and deleting the dashed portions of the red edges, as well as all red vertices; let  $\mathcal{S}_3$  be the new subdivision. The last operation has two effects on the set of faces. On one hand, it doubles the edges of each face of  $\mathcal{S}_2$ ; thus, these faces are always even-sided. On the other hand, it adds a new face around each vertex of  $\mathcal{S}_2$ , with a

number of edges equal to its degree. Hence, these faces are even-sided if and only if the faces of  $\mathcal{S}_1$  are even-sided. ◀



■ **Figure 13** Constructing the truncated dual of a convex subdivision of the sphere

Figure 14 shows two applications of Proposition 26. The two top SODs are swirlifications of a 6-trapezohedron and a truncated 6-antiprism; note that  $k$ -trapezohedron and  $k$ -antiprism are dual polyhedra. The two bottom SODs are swirlifications of a rhombic triacontahedron and a truncated icosidodecahedron; the rhombic triacontahedron and the icosidodecahedron are dual polyhedra.

## 6 Uniform SODs

We now turn to a class of SODs that generalizes the swirling ones.

► **Definition 27.** *A SOD is uniform if every arc blocks the same number of arcs.*

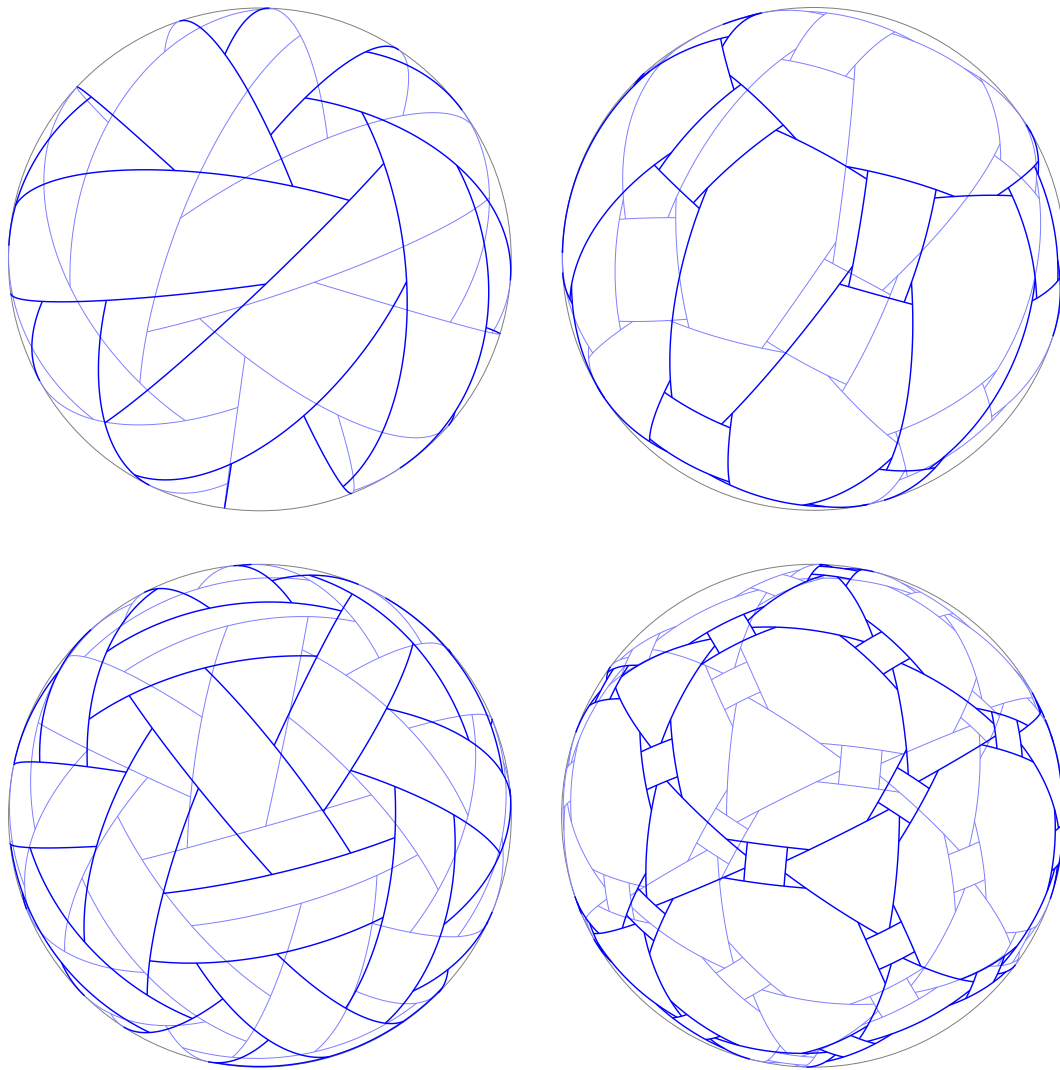
► **Proposition 28.** *For a SOD  $\mathcal{D}$ , the following are equivalent.*

1.  $\mathcal{D}$  is uniform.
2. Every arc of  $\mathcal{D}$  blocks exactly two arcs.
3. Every arc of  $\mathcal{D}$  blocks at least two arcs.
4. Every arc of  $\mathcal{D}$  blocks at most two arcs.

**Proof.** By Proposition 6, each arc hits exactly two distinct arcs. Hence, each arc blocks two arcs on average. Thus, if all arcs blocks the same number of arcs, this number must be two. For the same reason, if every arc blocks at most two arcs (or at least two arcs), it must block exactly two arcs. ◀

► **Proposition 29.** *Every uniform SOD is irreducible.*

**Proof.** Let  $\mathcal{D}$  be a uniform SOD, and assume that there is a proper subset of arcs  $\mathcal{D}' \subset \mathcal{D}$  that is itself a SOD. By Corollary 14,  $\mathcal{D}$  is connected; thus, removing arcs from  $\mathcal{D}$  causes some arcs to block fewer than two arcs. Since  $\mathcal{D}$  is uniform, it follows that the arcs of  $\mathcal{D}'$  block fewer than two arcs on average, contradicting Proposition 6. ◀



■ **Figure 14** Examples of the swirlification method developed in Section 5 to produce swirling SODs from convex polyhedra with a bipartite 1-skeleton (or, equivalently, from swirlable subdivisions of the unit sphere). The pictures show swirling SODs resulting from a 6-trapezohedron, a truncated 6-antiprism, a rhombic triacontahedron, and a truncated icosidodecahedron, respectively.

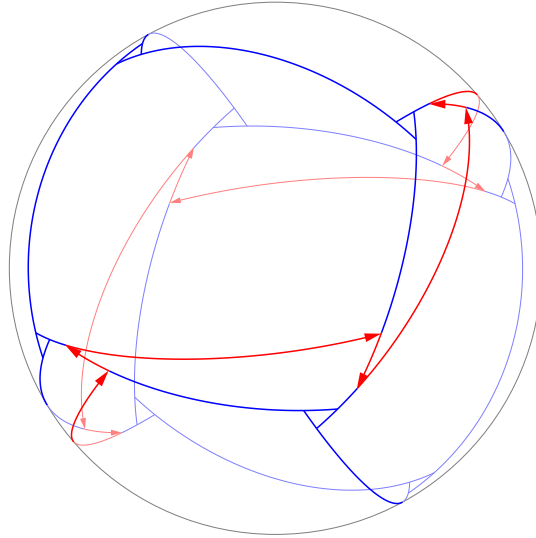
► **Corollary 30.** *In a uniform SOD, the eye of each swirl coincides with a single tile.*

**Proof.** If the interior of the eye of a swirl contains some arcs, then such arcs can be removed without violating the SOD axioms. Hence, such a SOD is not irreducible, and by Proposition 29 it cannot be uniform. ◀

► **Theorem 31.** *Every swirling SOD is uniform.*

**Proof.** In a swirling SOD, each arc  $a$  is part of two distinct swirls. By Theorem 18, these two swirls share no arcs other than  $a$ , and hence  $a$  must block one arc from each of them. Therefore, every arc in a swirling SOD blocks at least two arcs, and by Proposition 28 the SOD is uniform. ◀

The converse of Theorem 31 is not true in general, as Figure 15 shows.



■ **Figure 15** A uniform SOD that is not swirling

► **Definition 32.** An endpoint of an arc of a SOD is called a swirling vertex if it is incident to the eye of a swirl. A walk on a SOD is non-swirling if it does not touch swirling vertices and, whenever it touches the interior of an arc, it follows it until it reaches one of its endpoints, without touching any other arc along the way. A cyclic non-swirling walk is called a non-swirling cycle.

Observe that there is a non-swirling cycle that covers all the non-swirling vertices of the SOD in Figure 15 (drawn in red). As the next theorem shows, this is not a coincidence.

► **Theorem 33.** In a uniform SOD where no two arcs share an endpoint, all non-swirling vertices are covered by disjoint non-swirling cycles.

**Proof.** Suppose that no two arcs of a uniform SOD share an endpoint. Consider a non-swirling walk  $W$  terminating at a non-swirling vertex  $x_i$ , endpoint of an arc  $a_i$ , as Figure 16 shows. We will prove that  $W$  can be extended to a longer non-swirling walk in a unique way.

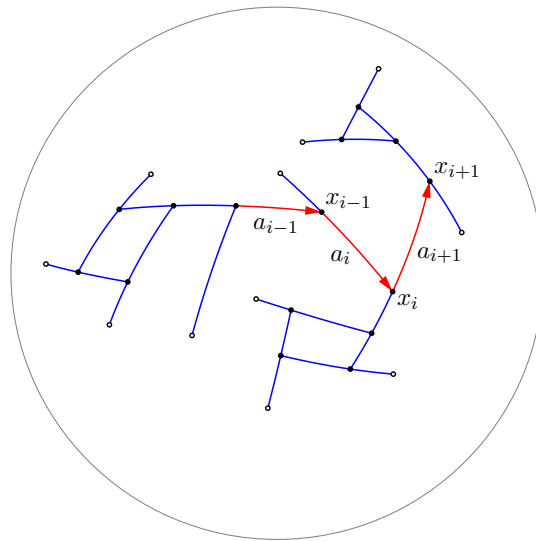
Let  $a_{i+1}$  be the arc that blocks  $a_i$  at  $x_i$ . Since exactly one arc other than  $a_i$  hits  $a_{i+1}$ , and it does so at an endpoint other than  $x_i$ , there is exactly one endpoint of  $a_{i+1}$ , say  $x_{i+1}$ , that can be reached from  $x_i$  without touching any arc other than  $a_{i+1}$ .

By definition of non-swirling walk,  $x_{i+1}$  can be used to extend  $W$  if and only if it is a non-swirling vertex. However, if  $x_{i+1}$  were incident to a swirl's eye  $E$ , then an arc of that swirl would either hit  $a_{i+1}$  between  $x_i$  and  $x_{i+1}$ , contradicting the fact that  $a_{i+1}$  blocks exactly two arcs, or it would hit  $a_{i+1}$  on the other side of  $x_i$ , implying that  $E$  contains the arc  $a_i$  in its interior, which contradicts Corollary 30.

Hence,  $W$  can be extended uniquely to a non-swirling walk. By a similar reasoning, we argue that  $W$  can also be uniquely extended backwards to a non-swirling walk. Thus,  $W$  is part of a unique non-swirling cycle. Now we conclude the proof by inductively repeating the same argument with any remaining non-swirling vertices. ◀

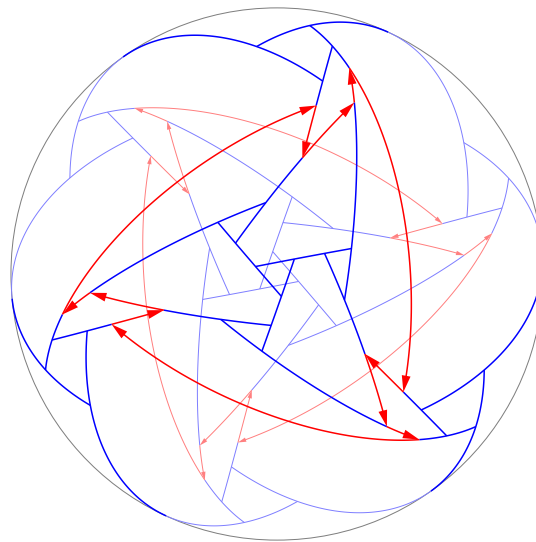
It is straightforward to extend Theorem 33 to “degenerate” uniform SODs where two arcs may share an endpoint. However, in this case the portions of arcs that do not contribute to swirls are only partitioned into edge-disjoint cycles (as opposed to vertex-disjoint cycles).





■ **Figure 16** Proof of Theorem 33: A non-swirling walk can be extended indefinitely.

We remark that we can construct uniform SODs with any number of unboundedly long non-swirling cycles. An example with two non-swirling cycles is shown in Figure 17.



■ **Figure 17** A uniform SOD with two non-swirling cycles

## 7 Conclusions

We introduced the theory of Spherical Occlusion Diagrams and studied their basic properties, while also discussing some applications to visibility-related problems in discrete and computational geometry.

Although we strongly believe Conjecture 5 to be true, i.e., not all irreducible SODs can be realized as polyhedra, a related and more subtle question can be asked, inspired by previous work on weaving patterns [1, 8]. Namely, whether for every SOD  $\mathcal{D}$  there is a *combinatorially*

equivalent SOD  $\mathcal{D}'$  and a polyhedron  $\mathcal{P}$  such that  $\mathcal{D}' = S_{\mathcal{P}}$ . In other words, does every class of combinatorially equivalent SODs contain a realizable instance?

We have introduced three noteworthy families of SODs: irreducible, uniform, and swirling. We proved that all swirling SODs are uniform, and all uniform SODs are irreducible. In the case of swirling SODs, we were able to characterize their swirl graphs as the 1-skeletons of even-sided convex polyhedra (Proposition 23). It remains an open problem to characterize the swirl graphs of other families of SODs. Theorem 33 is a step in this direction: We conjecture that the swirl graph of a uniform SOD can also be obtained from the 1-skeleton of an even-sided convex polyhedron, provided that the edges touched by a set of cycles in its dual graph are deleted (and vice versa).

The structural connection between swirling and uniform SODs revealed by Theorem 33 can also be taken a step further. It seems to be possible to systematically transform any uniform SOD into a swirling SOD by “sliding” the endpoints of some arcs along other arcs and “merging” coincident arcs. Making this observation rigorous is left as a direction for future work.

More generally, we may wonder which SODs can be transformed into swirling ones by sequences of elementary operations on arcs (defining suitable “elementary operations” is in itself an open problem). The SOD in Figure 9 shows that the question is not trivial. Indeed, this is the unique configuration of any SOD with eight or fewer arcs; since the SOD itself is not swirling, it cannot be transformed into a swirling one by means of operations that only rearrange or merge arcs.

Tóth has pointed out an interesting similarity between SODs and *one-sided rectangulations*, which are subdivision of an axis-aligned rectangle into axis-aligned rectangles with a property analogous to our axiom A3. It is known that any one-sided rectangulation is *area-universal*, i.e., any assignment of areas to its rectangles can be realized by a combinatorially equivalent rectangular layout [4, 6]. We wonder if a similar property holds for SODs, and to what extent the theory of one-sided rectangulations can provide insights for the study of SODs.

---

## References

- 1 Saugata Basu, Raghavan Dhandapani, and Richard Pollack. On the realizable weaving patterns of polynomial curves in  $\mathbb{R}^3$ . In *Proceedings of the 12th International Symposium on Graph Drawing (GD 2004)*, pages 36–42, 2004.
- 2 Nadia M. Benbernou, Erik D. Demaine, Martin L. Demaine, Anastasia Kurdia, Joseph O’Rourke, Godfried T. Toussaint, Jorge Urrutia, and Giovanni Viglietta. Edge-guarding orthogonal polyhedra. In *Proceedings of the 23rd Canadian Conference on Computational Geometry (CCCG 2011)*, pages 461–466, 2011.
- 3 Javier Cano, Csaba D. Tóth, Jorge Urrutia, and Giovanni Viglietta. Edge guards for polyhedra in three-space. *Computational Geometry: Theory and Applications*, 104:101859, 2022.
- 4 David Eppstein, Elena Mumford, Bettina Speckmann, and Kevin Verbeek. Area-universal and constrained rectangular layouts. *SIAM Journal on Computing*, 41(3):537–564, 2012.
- 5 Kimberly Kokado and Csaba D. Tóth. Nonrealizable planar and spherical occlusion diagrams. In *Proceedings of the 24th Japan Conference on Discrete and Computational Geometry, Graphs, and Games (JCDCGGG 2022)*, pages 60–61, 2022.
- 6 Arturo Merino and Torsten Mütze. Efficient generation of rectangulations via permutation languages. In *37th International Symposium on Computational Geometry (SoCG 2021)*, volume 189, pages 54:1–54:18, 2021.
- 7 Joseph O’Rourke. Visibility. In Jacob E. Goodman, Joseph O’Rourke, and Csaba D. Tóth, editors, *Handbook of discrete and computational geometry*, chapter 33, pages 875–896. CRC Press, 2017.

- 8 János Pach, Richard Pollack, and Emo Welzl. Weaving patterns of lines and line segments in space. *Algorithmica*, 9(6):561–571, 1993.
- 9 Csaba D. Tóth, Jorge Urrutia, and Giovanni Viglietta. Minimizing visible edges in polyhedra. In *Proceedings of the 23rd Thailand-Japan Conference on Discrete and Computational Geometry, Graphs, and Games (TJCDCGGG 2020+1)*, pages 70–71, 2021.
- 10 Csaba D. Tóth, Jorge Urrutia, and Giovanni Viglietta. Minimizing visible edges in polyhedra. *arXiv:2208.09702 [cs.CG]*, pages 1–19, 2022.
- 11 Giovanni Viglietta. Optimally guarding 2-reflex orthogonal polyhedra by reflex edge guards. *Computational Geometry: Theory and Applications*, 86:101589, 2020.
- 12 Giovanni Viglietta. A theory of spherical diagrams. In *Proceedings of the 34th Canadian Conference on Computational Geometry (CCCG 2022)*, pages 306–313, 2022.